Brazilian Journal of Medical and Biological Research (2023) 56: e12742, https://doi.org/10.1590/1414-431X2023e12742
ISSN 1414-431X Research Article

Brain glucose hypometabolism and hippocampal inflammation in Goto-Kakizaki rats

J.C.O. Borges[1*], V.A.B. Oliveira[1*], T.D.A. Serdan[1], F.L.R. Silva[1], C.S. Santos[1], J.R.B. Pauferro[1], A.S.F. Ribas[1], R. Manoel[1], A.C.G. Pereira[1], I.S. Correa[1], J.N.B. Pereira[2], R.B. Bazotte[3], A.C. Levada-Pires[1], T.C. Pithon-Curi[1], R. Gorjão[1], R. Curi[1,2], S.M. Hirabara[1], and L.N. Masi[1,4]

[1]Programa Interdisciplinar de Ciências da Saúde, Universidade Cruzeiro do Sul, São Paulo, SP, Brasil
[2]Seção de Produção de Imunobiológicos, Bioindustrial Centro, Instituto Butantan, São Paulo, SP, Brasil
[3]Programa de Pós-Graduação em Ciências Farmacêuticas, Departamento de Farmacologia e Terapêutica, Universidade Estadual de Maringá, Maringá, PR, Brasil
[4]Departamento de Ciências Fisiológicas, Centro de Ciências Biológicas, Universidade Federal de Santa Catarina, Florianópolis, SC, Brasil

Abstract

Brain glucose hypometabolism and neuroinflammation are early pathogenic manifestations in neurological disorders. Neuroinflammation may also disrupt leptin signaling, an adipokine that centrally regulates appetite and energy balance by acting on the hypothalamus and exerting neuroprotection in the hippocampus. The Goto-Kakizaki (GK) rat is a non-obese type 2 diabetes mellitus (T2DM) animal model used to investigate diabetes-associated molecular mechanisms without obesity jeopardizing effects. Wistar and GK rats received the maintenance adult rodent diet. Also, an additional control group of Wistar rats received a high-fat and high-sugar diet (HFHS) provided by free consumption of condensed milk. All diets and water were provided *ad libitum* for eight weeks. Brain glucose uptake was evaluated by 2-deoxy-2-[fluorine-18] fluoro-D-glucose under basal (saline administration) or stimulated (CL316,243, a selective β3-AR agonist) conditions. The animals were fasted for 10–12 h, anesthetized, and euthanized. The brain was quickly dissected, and the hippocampal area was sectioned and stored at –80°C in different tubes for protein and RNA analyses on the same animal. GK rats exhibited attenuated brain glucose uptake compared to Wistar animals and the HFHS group under basal conditions. Also, the hippocampus of GK rats displayed upregulated leptin receptor, IL-1β, and IL-6 gene expression and IL-1β and the subunit of the transcription factor NF-κB (p-p65) protein expression. No significant alterations were detected in the hippocampus of HFHS rats. Our data indicated that a genetic predisposition to T2DM has significant brain deteriorating features, including brain glucose hypometabolism, neuroinflammation, and leptin signaling disruption in the hippocampal area.

Key words: Insulin resistance; Cognitive disorders; Hyperglycemia; Hippocampus; Leptin; Goto-Kakizaki rats

Introduction

The prevalence of diabetes is increasing worldwide, and type 2 diabetes mellitus (T2DM) is the most prevalent form of this disease regardless of age, sex, and ethnicity (1). Genetic components and lifestyle factors, such as diet and physical activity, are the leading causes of insulin resistance (IR) and T2DM, which are usually associated with an obesity state (2). In addition to obesity, another critical factor contributing to the prevalence of IR and T2DM is the increase in longevity (1).

Approximately 80% of adult T2DM patients are overweight or obese; body weight reduction improves control of blood glucose levels. However, 10–15% of patients with T2DM are not obese (3) and exhibit hyperglycemic events more often with higher mortality (4). The Goto-Kakizaki (GK) rat is a non-obese T2DM animal model, which shows moderate hyperglycemia, glucose intolerance, peripheral IR, chronic inflammation, reduced pancreatic β-cell number, small intestine remodeling with local inflammation, and reduced intestinal transit (5–8). GK rats also present altered brain energy metabolism characterized by an impaired glutamate-glutamine cycle between neurons and astrocytes (9), cognitive dysfunction and

Correspondence: L.N. Masi: <laureane.masi@ufsc.br>

*These authors contributed equally to this study.

Received April 10, 2023 | *Accepted May 5, 2023*

neuroinflammation at six months of age (10), and higher levels of the Alzheimer's-related proteins p-tau and amyloid-β at 12.5 months of age (11). In this sense, GK rats allow researchers to investigate the T2DM-associated molecular mechanisms without the obesity-induced jeopardizing effects.

Cognitive dysfunction and neurodegenerative diseases such as Alzheimer's disease (AD), Parkinson's disease (PD), Huntington's disease, and epilepsy-related disorders (12) are frequent T2DM comorbidities (13). Despite the distinct etiologies of neurological diseases, they share common pathogenic manifestations, particularly brain glucose hypometabolism and neuroinflammation (14).

Interestingly, brain glucose hypometabolism precedes the clinical manifestations of some neurological diseases over the years, suggesting that it could be an early neurodegenerative diseases biomarker (14). Studies with 2-deoxy-2-[fluorine-18] fluoro-D-glucose integrated with computed tomography (18F-FDG PET/CT) imaging revealed a significant reduction in brain glucose metabolism in patients with mild cognitive impairment in early AD (15) and PD (16) stages.

Neuroinflammation is also present in the initial stages of these diseases. A previous study reported that neuroinflammation is initiated by microglia and astrocyte activation, releasing cytokines [e.g., interleukin (IL)-6 and IL-1β], which contributes to the inflammatory process that can lead to neural dysfunction and cell death (17). In brain cells, nuclear factor kappa B (NF-κB) is the main transcription factor of these pro-inflammatory cytokines. Cytokine expression depends on p65 subunit phosphorylation and translocation to the promoter region of the genes (18).

In T2DM animal models, cognitive deficits were primarily associated with impairments in the hippocampus (19). Like the hypothalamus and many brain areas, the hippocampus expresses leptin receptors essential to hippocampal synapses in this region (20) and protective actions such as neuronal apoptosis and neuronal degeneration (21). Leptin is principally synthesized in white adipose tissue, and plasma levels correlate directly to body fat content (22). Notably, genetically lean T2DM GK rats also present elevated plasma leptin concentrations (23). Leptin can cross the blood-brain barrier (BBB), and it has been shown that high leptin levels can lead to subsequent leptin resistance and low leptin levels, which are both associated with an increased risk of AD (24). Downregulated expression of leptin receptor mRNA and immunoreactivity has been detected in post-mortem AD tissue, suggesting the possible development of leptin resistance (25). GK rats also exhibited leptin resistance for the effect on food consumption (23) in the hypothalamic arcuate nucleus (26).

Plasma insulin and leptin concentrations, brain glucose metabolism, neuroinflammation, and leptin receptor expression in the hippocampus of GK rats fed the AIN-93-M diet were compared with Wistar rats fed the AIN-93-M diet, or Wistar rats fed a high-fat high-sugar diet (HFHS). We hypothesized that the predisposing genetic factors for T2DM produce more severe brain effects than an obesogenic diet.

Material and Methods

Ethics approval

All experimental procedures were previously approved by the Committee on Ethics in the Use of Animals at Cruzeiro do Sul University (protocol number 024/2017).

Experimental protocol

Briefly, 8-week-old male Wistar rats and non-obese T2DM GK rats (8) were housed in a room with a 12-h light/dark cycle, maintained at 23 ± 2°C, with circulating air. Each group of animals had free access to water and standard rodent chow (Quimtia™, Brazil) before the initiation of the experimental protocol. Wistar and GK rats received the maintenance adult rodent diet proposed by the American Institute of Nutrition (AIN-93-M) (27,28), i.e., a diet containing 70% carbohydrate, 20% protein, and 10% fat in energy; 3.85 kcal/g (Rhoster Company, Brazil). For comparative purpose, an additional control group of obese Wistar rats (HFHS group) was included. Obesity was induced by a high-fat (60% fat, 20% protein, and 20% carbohydrate in energy; 5.24 kcal/g; Rhoster Company) and high-sugar diet provided by free consumption of condensed milk (68% carbohydrate, 23% fat, and 9% protein in energy; 3.25 kcal/g, Italac, Brazil) (Figure 1). All diets and water were provided *ad libitum* for eight weeks. At 16 weeks of age, the animals underwent fasting for 10–12 h and were then anesthetized (10 mg/kg of xylazine and 75 mg/kg of ketamine) and euthanized. The brain was quickly dissected, and the hippocampal area was sectioned and stored at –80°C in different tubes for protein and RNA analysis on the same animal.

Food intake and caloric consumption

Food consumption of four to five animals per cage and the body weight of each rat were monitored weekly throughout the experimental protocol using a precision scale. The food intake was estimated by the total weekly consumption per cage (g) normalized by the number of animals in the cage (n) divided by the average body weight (g). Consumption of condensed milk by the HFHS group was also evaluated to calculate total food intake and caloric ingestion. The caloric consumption was calculated by the result obtained for food intake multiplied by the calories of the respective diet for AIN-93-M with 3.85 kcal/g or HFHS with 5.24 kcal/g.

Glucose tolerance test

After 56 days of the experimental diet, the animals were fasted for 12 h to evaluate glycemia. They received

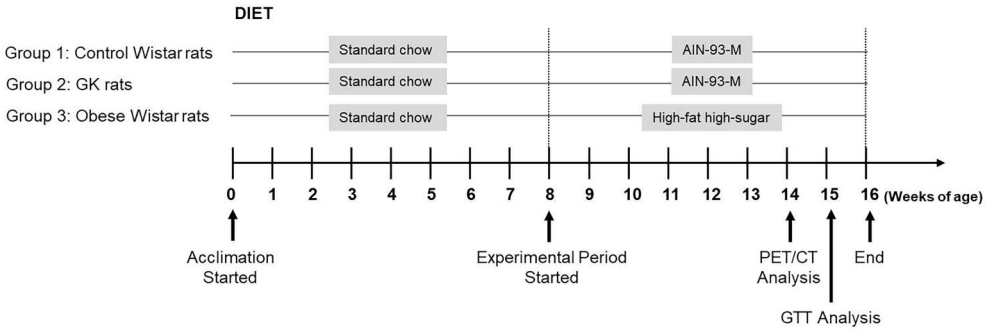

Figure 1. Experimental design used in the present study. Wistar and Goto-Kakizaki (GK) rats were fed a standard chow diet for eight weeks and then started to receive an experimental diet according to each group: 1) Control Wistar rats: Wistar rats fed an AIN-93-M diet (n=8); 2) GK rats: Goto-Kakizaki rats fed an AIN-93-M diet (n=8); and 3) obese Wistar rats: Wistar rats fed a high-fat high-sugar diet (n=8). GTT: glucose tolerance test; PET/CT: positron emission tomography and computed tomography.

an intraperitoneal (*ip*) injection of 2 g of D-glucose per kg body mass. Blood glucose was measured by strips in a glucometer (Accu-Chek Active, Roche, Switzerland) in the samples obtained from the animals' tails at time zero (fasted glycemia) and 15, 30, 60, and 90 min after glucose administration. The results for each animal were evaluated according to the area under the curve (AUC) for each group.

Determination of fasting plasma insulin and leptin concentrations

Commercially available enzyme-linked immunosorbent assay (ELISA) kits were used to measure the plasma insulin (Ins1 insulin ELISA kit, #RAB0904) and leptin (Rat Leptin ELISA kit, #RAB0335) concentrations following the manufacturer's instructions (Sigma-Aldrich, USA) in 12-h fasted rats.

Positron emission tomography with 18F-FDG PET/CT

18F-FDG PET/CT images were acquired after six weeks of the experimental diets using a small-animal PET Scanner (Triumph™-Gamma Medica-Ideas, USA). The animals were housed at the Nuclear Medicine Laboratory (LIM-43) facility, University of São Paulo, Brazil, for 24 h before the PET images. A bolus of 37–55 MBq of ^{18}F-FDG was administered in the penile vein under adrenergic stimulation or basal conditions. Under stimulated conditions, an intravenous injection of CL316,243 (1 mg/kg) was given 30 min before ^{18}F-FDG administration. In the basal state, animals received an intravenous saline injection. Images were acquired 45 min after the ^{18}F-FDG injection, with the animal under isoflurane inhalation anesthesia (1.5–3%). We selected polygonal regions of interest on coronal PET/CT brain slices. Mean standardized uptake values (SUVs) of target-to-background ratios from each region of interest were measured as indices of 18F-FDG uptake.

Hippocampus gene expression measurements by quantitative polymerase chain reaction (qPCR)

The hippocampal tissue was powdered in liquid nitrogen, and approximately 40 mg was homogenized in 1 mL of TRIZOL reagent (Invitrogen, USA) for total RNA extraction. The total RNA extract's concentration and purity (A260/A280 and A260/A230 ratios) were assessed using a NanoDrop 2000 (Thermo Fisher Scientific, Uniscience, Brazil). A High-Capacity cDNA Reverse Transcription Kit (Applied Biosystems, USA) was utilized to synthesize a new strand of cDNA for 1 μg of total RNA by reverse transcription. The QuantStudio 3 Real-time PCR system (Thermo Fisher Scientific, USA) was used to evaluate the mRNA expression by real-time qPCR using the fluorescent dye SYBR green (Applied Biosystems) and specific primers. The $2^{-\Delta\Delta CT}$ method with *Rplp0* as the reference gene was employed to quantify gene expression. The primer sequences included *IL-6*, NM_012589.2, forward CATTCTGTCTCGAGCCCACC, reverse GCTGGA AGTCTCTTGCGGAG; *IL-1β*, NM_031512.2, forward CAG CTTTCGACAGTGAGGAGA, reverse TGTCGAGATGCT GCTGTGAG; *Rplp0*, NM_022402.2, forward CCTTCCT CTTCGGACTTGGG, reverse CCTTCCTCTTCGGACTT GGG.

Hippocampal protein analysis by western blot

Pulverized hippocampus tissue (100 mg) was homogenized in RIPA-like buffer (500 μL; Hepes-KOH 20 mM, glycerol 25%, $MgCl_2$ 5 mM, EDTA 0.1 mM, KCl 520 mM, DTT 1 mM, PMSF 0.5 mM, NP-40 0.2%) containing protease inhibitor cocktail (#11836153001 Complete-Mini, Roche, Switzerland). Protein content was determined in the supernatant of tissue extract using a BCA kit (Thermo Scientific, USA), and Laemmli buffer was added to the samples. For each sample, 40 μg of total protein was loaded onto 10% polyacrylamide gels and subjected to SDS-PAGE. Following separation, the proteins in the gel

were transferred to nitrocellulose membranes using a semidry electrophoretic transfer apparatus (Transblot Turbo, Bio-Rad, USA). The membranes were washed, blocked in 5% skimmed milk for 1 h at room temperature and incubated with the specific primary antibodies, which included monoclonal anti-IL-1β (1:1000, ab9722, Abcam, UK), monoclonal anti-p-p65-NF-κB (1:1000, #3033, Cell Signaling, USA), monoclonal anti-amyloid-β (1:1000, ab 2539, Abcam), monoclonal anti-p-tau (1:1000, ab 109390, Abcam), and monoclonal anti-leptin receptor (1:1000,

Table 1. Body weight, food and calorie intake, glycemia, area under the curve (AUC) of the glucose tolerance test (GTT), and insulinemia of the study groups.

Measurements	Control Wistar rats	GK rats	Obese Wistar rats
Body weight gain (g)	279.6 ± 36.6	193.9 ± 12.4*#	332.6 ± 32.2*
Food intake/body weight (g/g)	0.36 ± 0.2	0.47 ± 0.2	0.34 ± 0.2
Calorie intake/body weight (kcal/g)	1.12 ± 0.4	1.52 ± 0.7	1.75 ± 0.8*
Fasted glycemia (mg/dL)	99.3 ± 12.1	186.8 ± 33.9*#	115.8 ± 11.9*
AUC of the GTT	1661 ± 7161	37007 ± 8310*#	20320 ± 4089
Fasted insulinemia (pg/mL)	0.68 ± 0.03	1.18 ± 0.49*	0.79 ± 0.21

Data reported as means ± SD. Control Wistar rats: Wistar rats fed an AIN-93-M diet (n=5); GK rats: Goto-Kakizaki rats fed an AIN-93-M diet (n=9); obese Wistar rats: Wistar rats fed a high-fat, high-sugar diet (HFHS) (n=6); *$P < 0.05$ compared with Control Wistar rats; #$P < 0.05$ compared with obese Wistar rats (one-way ANOVA followed by Tukey's post-test).

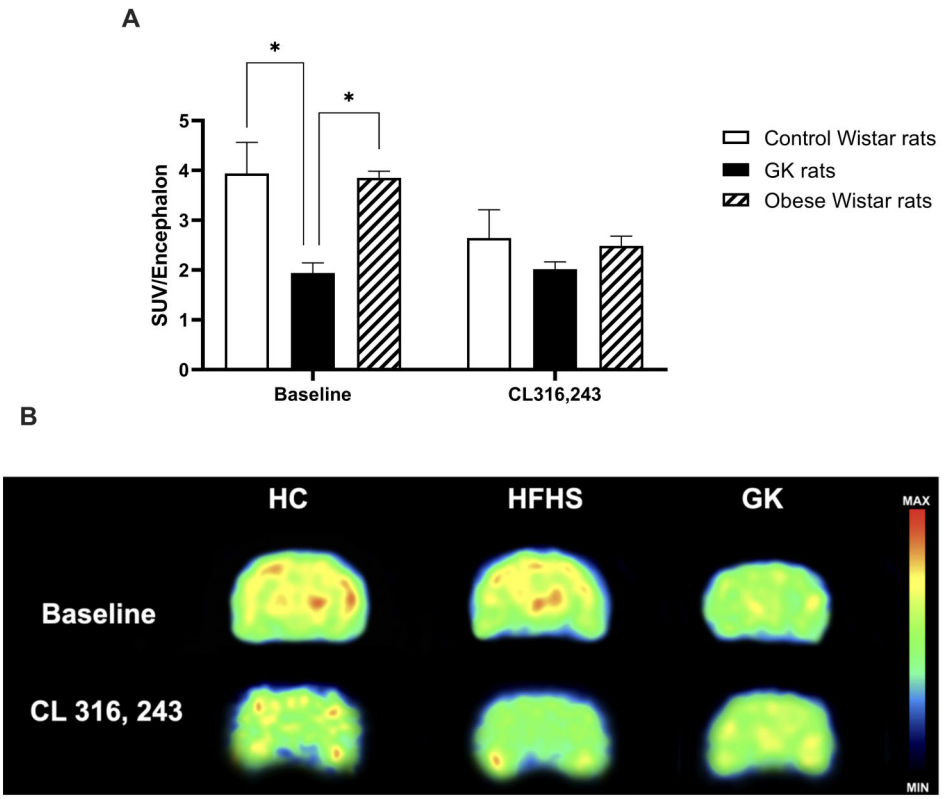

Figure 2. A, Brain activity evaluated by glucose uptake. Brain glucose 2-deoxy-2-[fluorine-18]fluoro-D-glucose standardized uptake value (SUV) detected by computed tomography after saline (baseline) and CL316,243 treatment. The animals were injected with saline (baseline) or CL316,243, a selective β3-AR agonist. **B**, The color in the images represents the intensity of glucose uptake in the brain according to the scale on the right of the image. Control Wistar rats (HC): Wistar rats fed an AIN-93-M diet (n=3); GK rats: Goto-Kakizaki rats fed an AIN-93-M diet (n=3); HFHS: Wistar rats fed a high-fat high-sugar diet (HFHS) (n=3). Data are reported as means ± SE. *$P < 0.05$ compared with GK rats (two-way ANOVA followed by Tukey's post-test).

#M00350, BoosterBio, USA), overnight at 4°C. The next day, the membranes were incubated with a secondary antibody conjugated to horseradish peroxidase, developed with an ECL kit (GE Healthcare Life Sciences, USA), and images were acquired using a gel documentation system (Amersham Biosciences, UK). Ponceau staining was used as an internal control (5). The ImageJ software (NIH, USA) was used to measure the relative band intensity.

Statistical analysis

Data are reported as means ± SD or ± SE. The normality was assessed with the Shapiro-Wilk test. Statistical analyses were conducted using one-way ANOVA followed by the Kruskal-Wallis post-test (for non-normal distribution data) or the Tukey post-test (for normal distribution data) (GraphPad Prism, version 7.0, USA) as indicated in each figure legend. The two-way ANOVA was used to interpret the positron emission tomography results. Results with $P < 0.05$ were considered statistically significant.

Results

As summarized in Table 1, the obese Wistar rats exhibited higher ($P < 0.05$) body mass gain (19%) and glycemia (17%) than Wistar rats. GK rats had reduced ($P < 0.05$) body weight gain (31 and 42%) and higher ($P < 0.05$) fasting glycemia (88 and 61%) compared to Wistar rats and the obese Wistar rats. There was no significant difference in Wistar rats fed an AIN-93-M diet or Wistar rats fed an HFHS diet in the AUCs of the GTT test. The AUC of GTT of GK rats was increased by 122 and 82%, respectively, compared to Wistar rats and the obese Wistar rats ($P < 0.05$). Additionally, plasma insulin levels were higher (73.5%, $P < 0.05$) in GK rats than in Wistar (Table 1).

The basal brain glucose uptake was significantly lower in GK rats than in Wistar rats (Figure 2A). The CL316,243 treatment did not significantly inhibit the 18F-FDG uptake in the three groups (Figure 2A).

In GK rats, plasma leptin levels and hippocampal leptin receptor protein expression were increased by 2.4-fold ($P < 0.05$) compared to Wistar rats (Figure 3A and B, respectively).

Concerning inflammatory cytokine, IL-1β and IL-6 expressions were upregulated (7-fold, $P < 0.05$) in the hippocampus of GK rats compared to the Wistar and the obese Wistar rats (Figure 4A and B). The hippocampal IL-1β protein content of GK rats was also increased ($P < 0.05$) by 66 and 47% compared to Wistar rats and the obese Wistar rats, respectively (Figure 4C). The phosphorylation of the p65 subunit in the NF-κB transcription factor was higher (37%; P=0.0658) in GK compared to Wistar rats (Figure 4D). The tau and amyloid-β brain protein expression levels were not different among the three groups (data not shown).

Discussion

GK rats had less body weight gain, hyperglycemia, hyperinsulinemia, hyperleptinemia, glucose intolerance, brain glucose hypometabolism, increased hippocampal IL-6 and IL-1β mRNA expressions, higher IL-1β protein expression, expressive increase in the transcription factor subunit p65-NF-κB, and higher leptin receptor protein

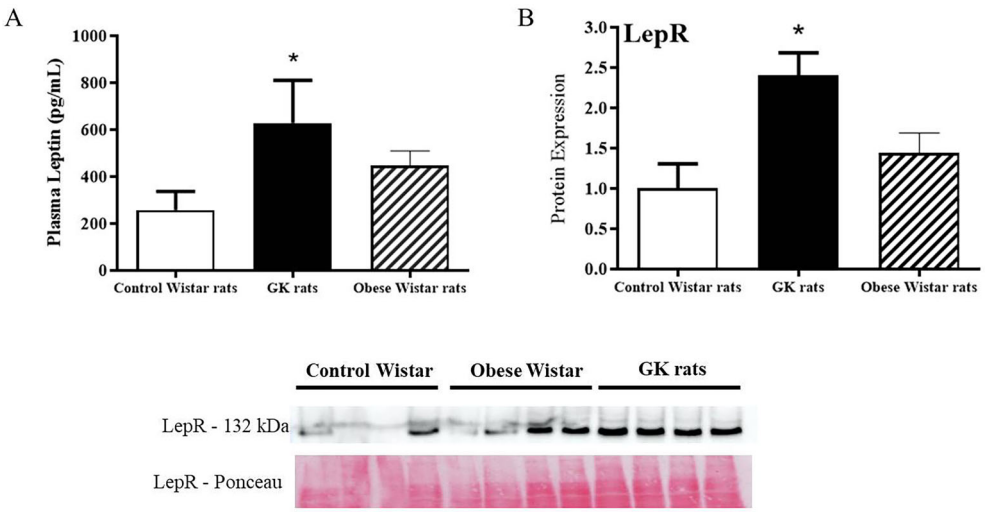

Figure 3. Plasma leptin (**A**) and protein expression of leptin receptor (LepR) (**B**) in the hippocampus of Control Wistar rats or GK (Goto-Kakizaki) rats fed an AIN-93-M diet or obese Wistar rats fed the high-fat high-sugar diet (HFHS) for eight weeks, as assessed by immunoblotting. Bottom figure: western blot image. The data are reported as means ± SE for n=8 rats in each group. *$P < 0.05$ *vs* Control Wistar rats (one-way ANOVA followed by Tukey's post-test).

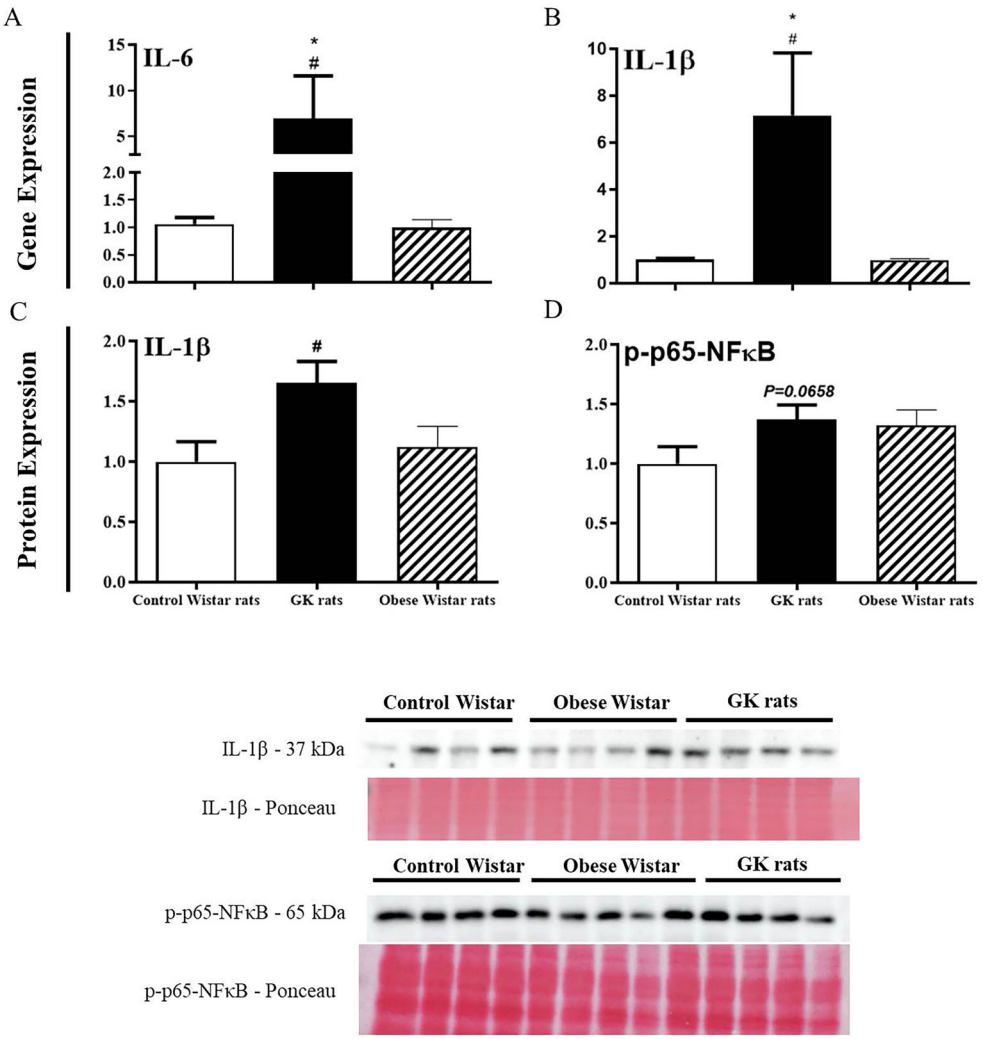

Figure 4. Hippocampus gene expression of interleukin(IL)-6 (**A**) and IL-1β (**B**) and protein expression of IL-1β (**C**) and p-p65-NFκB (**D**) in Control Wistar rats and GK (Goto-Kakizaki) rats fed an AIN-93-M diet or obese Wistar rats fed the high-fat high-sugar diet (HFHS) for eight weeks, as assessed by immunoblotting (bottom figure). The data are reported as means ± SE. Control Wistar rats (n=8), GK rats (n=4), and obese Wistar rats (n=7). *$P < 0.05$ compared with Control Wistar rats; #$P < 0.05$ compared with obese Wistar rats, using one-way ANOVA followed by Kruskal-Wallis post-test (gene expression analysis) or Tukey's post-test (protein expression analysis).

expression compared to Wistar rats. On the other hand, an obesogenic diet rich in fat and sugar (HFHS) for eight weeks induced higher body weight gain and hyperglycemia, with no significant alterations in the hippocampus of Wistar rats (Figure 5). Thus, a genetic factor was determinant in the evident brain effects observed in GK rats. A limitation of this study was that GK rats fed a HFHS were not included.

Body weight results were in agreement with previous studies (5,8) demonstrating higher body mass gain in 16-week-old Wistar rats fed the same HFHS diet for eight weeks and lower body mass gain in GK rats of the same age evaluated for the same period. The observation that GK rats gained less weight than Wistar rats despite similar energy intake could be explained by a higher metabolic rate in these animals, as reported by Landersdorfer et al. (23).

The eight-week HFHS diet induced hyperglycemia compared to the AIN-93 diet in Wistar rats. High-fat diets are commonly used in obesity-induced diabetes animal models (5,8,29). The palatability of the diets interferes with the amount consumed, contributing to the generation of adverse metabolic effects (29).

At four weeks of age, the GK rats already exhibit fasting hyperglycemia (30). Moreover, glycemic alterations, glucose intolerance, IR, and hyperinsulinemia

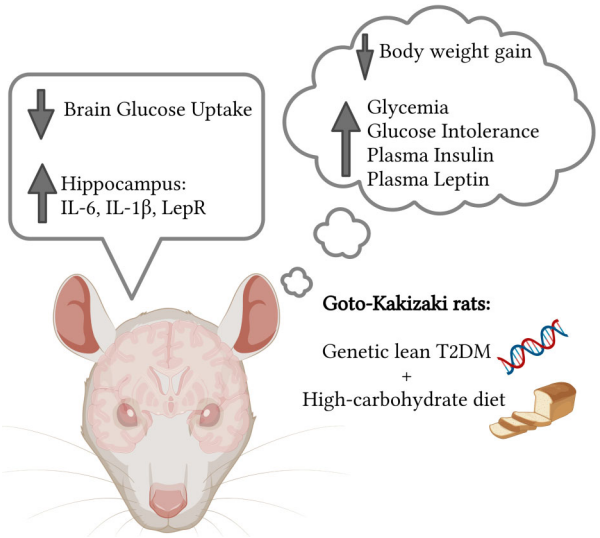

Figure 5. Summary of the results obtained in Goto-Kakizaki male rats fed an AIN-93-M diet. T2DM: type 2 diabetes mellitus; IL: interleukin; LepR: leptin receptor.

persist during adulthood at 16 weeks of age in GK rats (30), consistent with our previous studies (5,8).

Glucose is the primary fuel for the brain, and brain glucose hypometabolism is one of the most prominent features in cognitive dysfunction and AD patients (12). Although still controversial, this may occur more than a decade before the clinical onset of AD and is most evident in individuals that carry an APOE4 allele or with a positive family history of dementia (31). Disrupted cerebral glucose metabolism is visible using 18F-FDG PET/CT, and we showed a significant decrease in brain glucose uptake in GK rats compared to Wistar rats and the obese Wistar rats. Although the precise mechanism remains unclear, T2DM can exacerbate neurodegenerative processes. Notably, the hypometabolic brain pattern is one of the earliest pathologic events in AD (31,32).

GK rats also exhibit lower leptin receptor expression in the hippocampus, elevated plasma leptin levels, and leptin intolerance, as described by others (23,26). Leptin is produced in the white adipose tissue (22). It mediates feeding responses and energy metabolism accessing the hypothalamic neural circuits, but it has also been found to be neuroprotective in the hippocampus (21). Leptin resistance, reported in obese and IR rats, has been associated with a reduced ability of leptin to cross the blood-brain barrier (33) with consequent low activation of the long form of the leptin receptor (ObRb), which is encoded by the diabetes gene (db) (34) and highly expressed in the hippocampus.

T2DM involves neuroinflammation caused by the activation of brain microglia and astrocytes, further contributing to neuronal loss (35). The hypothesis proposing neuroinflammation as one of the key mechanisms of AD pathogenesis was introduced more than 30 years ago (36). Greenwood and Winocur (37) reported that Long-Evans rats fed a high-fat diet based on lard had memory and learning deficits derived from hippocampal alterations (37). Herein, GK rats had upregulated mRNA expression of the pro-inflammatory cytokines IL-6 and IL-1β and increased IL-1β and pro-inflammatory transcription factor p-p65-NFκB protein expression. GK rats submitted to oral administration of acrylamide at 1 mg/kg body weight for eight weeks presented significantly aggravated diabetes-associated cognitive dysfunction and increased IL-1β and IL-6 content after astrocyte and microglia activation, which exacerbated neuroinflammation (38). These inflammatory processes alter brain functions, predisposing patients to mood disorders that can impair cognition (39).

A general hypometabolism of glucose in the brain has been suggested to reduce activities at neuron synapses and to induce accumulation of key proteins involved in AD development, including beta amyloid and tau proteins (40). Additionally, insulin and leptin resistance can potentially exacerbate the dysregulation in brain glucose and lipid metabolism, contributing to increased neuroinflammation and neurodegeneration processes (35,40). GK rats are a well-described model of T2DM, which present insulin resistance and chronic and systemic inflammation (5,8). In this study, we demonstrated that these animals also present impaired brain glucose metabolism, increased neuroinflammation, and disrupted leptin signaling, which are early pathogenic characteristics of neurological disorders, including AD disease.

Our study is the first to demonstrate that GK rats, a non-obese animal model of T2DM, can be a potential model to evaluate several abnormalities related to the development of neurodegenerative and neurological diseases. These abnormalities include impaired glucose uptake and metabolism, elevated neuroinflammation, insulin resistance, and disrupted leptin function. Since patients with T2DM present an elevated risk for the development of several brain disorders, including cognitive function loss and dementia, two important and frequent disorders observed in patients with AD, additional studies are required to observe if non-obese T2DM patients also present the abnormalities observed in our study, aiming to comprehend the underlying mechanisms involved in this process and to evaluate potential strategies for prevention and/or therapy of these neurological abnormalities.

Conclusion

The genetic predisposition of GK rats resulted in massive brain dysfunction effects, evidenced by brain glucose hypometabolism, neuroinflammation, and leptin signaling disruption in the hippocampal area. Hippocampal neuroinflammation without alterations in AD-associated neuronal proteins indicates that this event precedes neurodegeneration.

Acknowledgments

The authors gratefully acknowledge Caroline Cristiano Real Gregório, PhD. and Daniele de Paula Faria, PhD. from the Laboratory of Nuclear Medicine of the University of São Paulo (LIM-43) for support with the PET-CT analysis. We thank Dr. Maria Elizabeth Pereira Passos for her technical assistance. This study was supported by the São Paulo State Research Foundation (FAPESP grants 2018/09868-7, 2019/25892-9, and 2021/02829-9), Coordination for the Improvement of Higher-Level Personnel (CAPES; Finance Code 001), and the National Council for Scientific and Technological Development (CNPq).

References

1. Magliano DJ, Boyko EJ. IDF Diabetes Atlas 10th edition scientific committee. IDF DIABETES ATLAS [Internet]. 10th ed. Brussels: International Diabetes Federation; 2021.
2. Kahn SE, Cooper ME, Del Prato S. Pathophysiology and treatment of type 2 diabetes: perspectives on the past, present, and future. *Lancet* 2014; 38: 1068–1083, doi: 10.1016/S0140-6736(13)62154-6.
3. Kashima S, Inoue K, Matsumoto M, Akimoto K. Prevalence and characteristics of non-obese diabetes in Japanese men and women: the Yuport Medical Checkup Center Study. *J Diabetes* 2015; 7: 523–530, doi: 10.1111/1753-0407.12213.
4. Hartman YAW, Jansen HJ, Hopman MTE, Tack CJ, Thijssen DHJ. Insulin-associated weight gain in type 2 diabetes is associated with increases in sedentary behavior. *Diabetes Care* 2017; 40: e120–e121, doi: 10.2337/dc17-0787.
5. Kuwabara WMT, Panveloski-Costa AC, Yokota CNF, Pereira JNB, Macini Filho J, Torres RP, et al. Comparison of Goto-Kakizaki rats and high fat diet-induced obese rats: are they reliable models to study type 2 diabetes mellitus? *PLoS One* 2017; 12: e0189622, doi: 10.1371/journal.pone.0189622.
6. Panveloski-Costa AC, Kuwabara WMT, Munhoz AC, Lucena CF, Curi R, Carpinelli AR, et al. The insulin resistance is reversed by exogenous 3,5,3'triiodothyronine in type 2 diabetic Goto-Kakizaki rats by an inflammatory-independent pathway. *Endocrine* 2020; 68: 287–295, doi: 10.1007/s12020-020-02208-5.
7. Pereira JNB, Murata GM, Sato FT, Marosti AR, Carvalho CRO, Curi R. Small intestine remodeling in male Goto-Kakizaki rats. *Physiol Rep* 2021; 9: 1–16, doi: 10.14814/phy2.14755.
8. Serdan TDA, Masi LN, Pereira JNB, Rodrigues LE, Alecrim AL, Scervino MVM, et al. Impaired brown adipose tissue is differentially modulated in insulin-resistant obese wistar and type 2 diabetic Goto-Kakizaki rats. *Biomed Pharmacother* 2021; 142: 112019, doi: 10.1016/j.biopha.2021.112019.
9. Girault FM, Sonnay S, Gruetter R, Duarte JMN. Alterations of brain energy metabolism in type 2 diabetic Goto-Kakizaki rats measured *in vivo* by ^{13}c magnetic resonance spectroscopy. *Neurotox Res* 2019; 36: 268–278, doi: 10.1007/s12640-017-9821-y.
10. Tian Z, Ren N, Wang J, Zhang D, Zhou Y. Ginsenoside ameliorates cognitive dysfunction in type 2 diabetic Goto-Kakizaki rats. *Med Sci Monit* 2018; 24: 3922–3928, doi: 10.12659/MSM.907417.
11. Pintana H, Apaijai N, Kerdphoo S, Pratchayasakul W, Sripetchwandee J, Suntornsaratoon P, et al. Hyperglycemia induced the Alzheimer's proteins and promoted loss of synaptic proteins in advanced-age female Goto-Kakizaki (GK) rats. *Neurosci Lett* 2017; 655: 41–45, doi: 10.1016/j.neulet.2017.06.041.
12. Biessels GJ, Despa F. Cognitive decline and dementia in diabetes mellitus: mechanisms and clinical implications. *Nat Rev Endocrinol* 2018; 14: 591–604, doi: 10.1038/s41574-018-0048-7.
13. Srikanth V, Sinclair AJ, Hill-Briggs F, Moran C, Biessels GJ. Type 2 diabetes and cognitive dysfunction-towards effective management of both comorbidities. *Lancet Diabetes Endocrinol* 2020; 8: 535–545, doi: 10.1016/S2213-8587(20)30118-2.
14. Blázquez E, Hurtado-Carneiro V, LeBaut-Ayuso Y, Velázquez E, García-García L, Gómez-Oliver F, et al. Significance of brain glucose hypometabolism, altered insulin signal transduction, and insulin resistance in several neurological diseases. *Front Endocrinol (Lausanne)* 2022; 13: 873301, doi: 10.3389/fendo.2022.873301.
15. Mosconi L, Pupi A, De Leon MJ. Brain glucose hypometabolism and oxidative stress in preclinical Alzheimer's disease. *Ann NY Acad Sci* 2008; 1147: 180–195, doi: 10.1196/annals.1427.007.
16. Xu Y, Wei X, Liu X, Liao J, Lin J, Zhu C, et al. Low cerebral glucose metabolism: a potential predictor for the severity of vascular parkinsonism and Parkinson's disease. *Aging Dis* 2015; 6: 426–436, doi: 10.14336/AD.2015.0204.
17. Zilberter Y, Zilberter M. The vicious circle of hypometabolism in neurodegenerative diseases: ways and mechanisms of metabolic correction. *J Neurosci Res* 2017; 95: 2217–2235, doi: 10.1002/jnr.24064.
18. Kempuraj D, Thangavel R, Natteru PA, Selvakumar GP, Saeed D, Zahoor H, et al. Neuroinflammation induces neurodegeneration. *J Neurol Neurosurg Spine* 2016; 1: 1003.
19. Bonds JA, Shetti A, Bheri A, Chen Z, Disouky A, Tai L, et al. Depletion of caveolin-1 in type 2 diabetes model induces Alzheimer's disease pathology precursors. *J Neurosci* 2019; 39: 8576–8583, doi: 10.1523/JNEUROSCI.0730-19.2019.
20. Shanley LJ, Irving AJ, Rae MG, Ashford ML, Harvey J. Leptin inhibits rat hippocampal neurons via activation of large conductance calcium-activated K+ channels. *Nat Neurosci* 2002; 5: 299–300, doi: 10.1038/nn824.
21. McGregor G, Harvey J. Regulation of hippocampal synaptic function by the metabolic hormone, leptin: implications for health and neurodegenerative disease. *Front Cell Neurosci* 2018; 12: 340, doi: 10.3389/fncel.2018.00340.
22. Considine RV, Sinha MK, Heiman ML, Kriauciunas A, Stephens TW, Nyce MR, et al. Serum immunoreactive-leptin concentrations in normal-weight and obese humans.

N Engl J Med 1996; 334: 292–295, doi: 10.1056/NEJM199602013340503.
23. Landersdorfer CB, DuBois DC, Almon RR, Jusko WJ. Mechanism-based modeling of nutritional and leptin influences on growth in normal and type 2 diabetic rats. *J Pharmacol Exp Ther* 2009; 328: 644–651, doi: 10.1124/jpet.108.144766.
24. Friedman EJ, Young K, Asif D, Jutla I, Liang M, Wilson S, et al. Alzheimer's disease neuroimaging initiative. Directed progression brain networks in Alzheimer's disease: properties and classification. *Brain Connect* 2014; 4: 384–393, doi: 10.1089/brain.2014.0235.
25. Maioli S, Lodeiro M, Merino-Serrais P, Falahati F, Khan W, Puerta E, et al. Alzheimer's disease neuroimaging initiative. Alterations in brain leptin signalling in spite of unchanged CSF leptin levels in Alzheimer's disease. *Aging Cell* 2015; 14: 122–129, doi: 10.1111/acel.12281.
26. Maekawa F, Fujiwara K, Kohno D, Kuramochi M, Kurita H, Yada T. Young adult-specific hyperphagia in diabetic Goto-kakizaki rats is associated with leptin resistance and elevation of neuropeptide Y mRNA in the arcuate nucleus. *J Neuroendocrinol* 2006; 18: 748–756, doi: 10.1111/j.1365-2826.2006.01470.x.
27. Reeves PG, Nielsen FH, Fahey Jr GC. AIN-93 purified diets for laboratory rodents: final report of the American Institute of Nutrition ad hoc writing committee on the reformulation of the AIN-76A rodent diet. *J Nutr* 1993; 123: 1939–1951, doi: 10.1093/jn/123.11.1939.
28. Antunes MM, Godoy G, de Almeida-Souza CB, da Rocha BA, da Silva-Santi LG, Masi LN, et al. A high-carbohydrate diet induces greater inflammation than a high-fat diet in mouse skeletal muscle. *Braz J Med Biol Res* 2020; 53: e9039, doi: 10.1590/1414-431x20199039.
29. Masi LN, Martins AR, Crisma AR, do Amaral CL, Davanso MR, Serdan TDA, et al. Combination of a high-fat diet with sweetened condensed milk exacerbates inflammation and insulin resistance induced by each separately in mice. *Sci Rep* 2017; 7: 3937, doi: 10.1038/s41598-017-04308-1.
30. Movassat J, Bailbé D, Lubrano-Berthelier C, Picarel-Blanchot F, Bertin E, Mourot J, et al. Follow-up of GK rats during prediabetes highlights increased insulin action and fat deposition despite low insulin secretion. *Am J Physiol Endocrinol Metab* 2008; 294: E168–E175, doi: 10.1152/ajpendo.00501.2007.
31. Bourgneuf C, Bailbé D, Lamazière A, Dupont C, Moldes M, Farabos D, et al. The Goto-Kakizaki rat is a spontaneous prototypical rodent model of polycystic ovary syndrome. *Nat Commun* 2021; 12: 1064, doi: 10.1038/s41467-021-21308-y.
32. Sperling R. Potential of functional MRI as a biomarker in early Alzheimer's disease. *Neurobiol Aging* 2011; 32: S37–S43, doi: 10.1016/j.neurobiolaging.2011.09.009.
33. Izquierdo AG, Crujeiras AB, Casanueva FF, Carreira MC. Leptin, obesity, and leptin resistance: where are we 25 years later? *Nutrients* 2019; 11: 2704, doi: 10.3390/nu11112704.
34. Tartaglia LA, Dembski M, Weng X, Deng N, Culpepper J, Devos R, et al. Identification and expression cloning of a leptin receptor, OB-R. *Cell* 1995; 83: 1263–1271, doi: 10.1016/0092-8674(95)90151-5.
35. Xu W, Caracciolo B, Wang HX, Winblad B, Bäckman L, Qiu C, et al. Accelerated progression from mild cognitive impairment to dementia in people with diabetes. *Diabetes* 2010; 59: 2928–2935, doi: 10.2337/db10-0539.
36. Hashioka S, Wu Z, Klegeris A. Glia-driven neuroinflammation and systemic inflammation in Alzheimer's disease. *Curr Neuropharmacol* 2021; 19: 908–924, doi: 10.2174/1570159X18666201111104509.
37. Greenwood CE, Winocur G. Learning and memory impairment in rats fed a high saturated fat diet. *Behav Neural Biol* 1990; 53: 74–87, doi: 10.1016/0163-1047(90)90831-P.
38. Quan W, Li M, Jiao Y, Zeng M, He Z, Shen Q, et al. Effect of dietary exposure to acrylamide on diabetes-associated cognitive dysfunction from the perspectives of oxidative damage, neuroinflammation, and metabolic disorders. *J Agric Food Chem* 2022; 70: 4445–4456, doi: 10.1021/acs.jafc.2c00662.
39. Kraynak TE, Marsland AL, Wager TD, Gianaros PJ. Functional neuroanatomy of peripheral inflammatory physiology: a meta-analysis of human neuroimaging studies. *Neurosci Biobehav Rev* 2018; 94: 76–92, doi: 10.1016/j.neubiorev.2018.07.013.
40. Ryu JC, Zimmer ER, Rosa-Neto P, Yoon SO. Consequences of metabolic disruption in Alzheimer's disease pathology. *Neurotherapeutics* 2019; 16: 600–610, doi: 10.1007/s13311-019-00755-y.